the FEBS Journal

The benzophenanthridine alkaloid sanguinarine perturbs microtubule assembly dynamics through tubulin binding

A possible mechanism for its antiproliferative activity

Manu Lopus and Dulal Panda

School of Biosciences and Bioengineering, Indian Institute of Technology Bombay, India

Keywords
cancer chemotherapy; microtubules; mitosis; sanguinarine; tubulin

Correspondence
D. Panda, School of Biosciences and Bioengineering, Indian Institute of Technology Bombay, Powai, Mumbai 400 076, India
Fax: +91 22 25723480
Tel: +91 22 25767838
E-mail: panda@iitb.ac.in

(Received 11 January 2006, revised 2 March 2006, accepted 13 March 2006)

doi:10.1111/j.1742-4658.2006.05227.x

Sanguinarine has been shown to inhibit proliferation of several types of human cancer cell including multidrug-resistant cells, whereas it has minimal cytotoxicity against normal cells such as neutrophils and keratinocytes. By analyzing the antiproliferative activity of sanguinarine in relation to its effects on mitosis and microtubule assembly, we found that it inhibits cancer cell proliferation by a novel mechanism. It inhibited HeLa cell proliferation with a half-maximal inhibitory concentration of 1.6 ± 0.1 μM. In its lower effective inhibitory concentration range, sanguinarine depolymerized microtubules of both interphase and mitotic cells and perturbed chromosome organization in mitotic HeLa cells. At concentrations of 2 μM, it induced bundling of interphase microtubules and formation of granular tubulin aggregates. A brief exposure of HeLa cells to sanguinarine caused irreversible depolymerization of the microtubules, inhibited cell proliferation, and induced cell death. However, in contrast with several other microtubule-depolymerizing agents, sanguinarine did not arrest cell cycle progression at mitosis. *In vitro*, low concentrations of sanguinarine inhibited microtubule assembly. At higher concentrations (> 40 μM), it altered polymer morphology. Further, it induced aggregation of tubulin in the presence of microtubule-associated proteins. The binding of sanguinarine to tubulin induces conformational changes in tubulin. Together, the results suggest that sanguinarine inhibits cell proliferation at least in part by perturbing microtubule assembly dynamics.

Microtubules are dynamic polymers composed of tubulin dimers. They perform a variety of cellular functions, including cell division, maintenance of cell shape and structure, and cell signaling [1–4]. They are important drug targets in several types of cancer. Microtubule-targeted agents including paclitaxel, vinblastine and estramustine have been successfully used in cancer chemotherapy, either as single agents or in combinations. Many such compounds are undergoing clinical trials [5–8].

The integrity of microtubules is considered essential for the faithful segregation of chromosomes during mitosis [3,8]. Most of the microtubule inhibitors, including nocodazole, vinblastine, LY290181, cryptophycin-52, benomyl and griseofulvin, inhibit cell cycle progression at mitosis [9–15]. These agents have been shown to inhibit mitosis by selectively perturbing spindle microtubule function at drug concentrations lower than those required to depolymerize interphase microtubules. For example, at their half-maximal antiproliferative concentrations (IC_{50}), benomyl, vinblastine, griseofulvin and cryptophycin-52 induce little depolymerization of interphase microtubules, but they arrest cells at the metaphase/anaphase transition and induce cell death [7,8,12,14,15]. Although mitotic arrest is the common mechanism for microtubule-targeted drugs,

Abbreviations
ANS, 1-anilinonaphthalene-8-sulfonic acid; IC_{50}, half-maximal inhibitory concentration; MAP, microtubule-associated protein.

exceptions to this have also been reported. For instance, halogenated derivatives of acetamidobenzoyl ethyl ester were found to depolymerize cellular microtubules and to arrest cells at the G_1/S transition, indicating that antitubulin agents can inhibit cell proliferation without arresting cells at mitosis [16]. In addition, it was shown that indanocine, a microtubule-depolymerizing agent, inhibits proliferation of certain types of noncycling tumor cell at G_0/G_1 phase [17].

Sanguinarine (13-methyl-[1,3]-benzodioxolo[5,6-c]-1,3-dioxolo-[4,5-i]-phenanthridinium chloride) (Fig. 1), a benzophenanthridine alkaloid derived from the plant *Sanguinaria canadensis*, has been shown to have antimicrobial, anti-inflammatory, antioxidant, and anticancer activities [18–27]. It was reported to inhibit proliferation of different types of cancer cell, including human prostate carcinoma cells (LNCaP, PC-3 and DU145), multidrug-resistant uterine cervical carcinoma cells, human epidermoid carcinoma A431 cells, human erythroleukemia K562 cells, and the premalignant cell-line HaCaT [23,24]. However, sanguinarine was found to be less toxic towards normal cells such as normal human epidermal keratinocytes [20]. It inhibits cell cycle progression at several stages of the cell cycle including G_0/G_1 and G_1/S [25]. Several mechanisms, including upregulation of pro-apoptotic Bax, downregulation of the antiapoptotic protein Bcl2, inhibition of mitogen-activated protein kinase phosphatase-1 and nuclear factor kappaB (NF-κB), and suppression of vascular endothelial growth factor-mediated angiogenesis have been proposed to explain the antiproliferative activities of this alkaloid [22–28]. Further, it has been shown that sanguinarine binds to tubulin, and this inhibits the binding of colchicine to tubulin [29]. In addition, sanguinarine has been shown to depolymerize microtubules in HeLa cells [21] and inhibit tubulin assembly *in vitro* [29]. However, how sanguinarine inhibits microtubule assembly is not clear, and the interaction of sanguinarine with cellular microtubules in relation to its antiproliferative activity is not understood. In this study, we examined the antiproliferative effects of sanguinarine in relation to its ability to perturb mitosis and microtubule assembly.

We found that sanguinarine inhibited microtubule assembly both *in vitro* and in cells and that the antiproliferative activity of sanguinarine correlates well with its ability to depolymerize cellular microtubules. However, it did not inhibit mitosis, indicating that its antiproliferative mechanism of action is distinct from most of the microtubule-targeted antimitotic agents. The results indicate that sanguinarine inhibits cell proliferation at least in part by depolymerizing cellular microtubules. We also suggest a mechanism that may explain the inhibitory effects of sanguinarine on microtubule assembly.

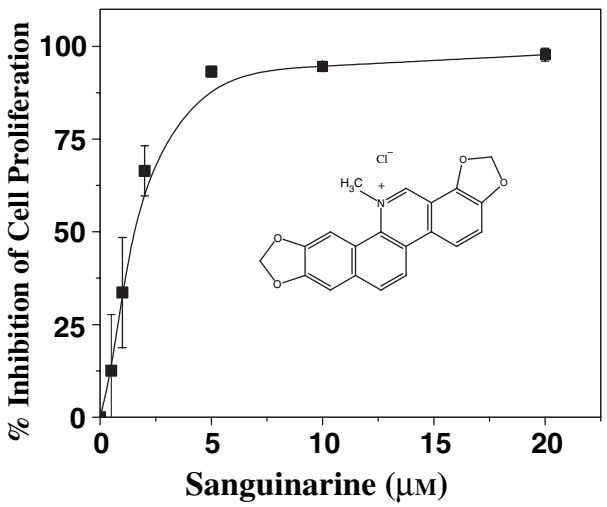

Fig. 1. Inhibition of HeLa cell proliferation by sanguinarine. The effect of sanguinarine on HeLa cell proliferation was determined by measuring A_{550} using sulforhodamine B as described in Experimental procedures. The chemical structure of sanguinarine {13-methyl-[1,3]-benzodioxolo-[5,6-c]-1,3-dioxolo-[4,5-i]-phenanthridinium} is shown in the inset.

Results

Sanguinarine depolymerized HeLa cell microtubules and disorganized mitotic chromosomes

We first wanted to analyze the antiproliferative actions of sanguinarine in HeLa cells. Sanguinarine inhibited HeLa cell proliferation in a concentration-dependent fashion with IC50 1.6 ± 0.1 μM (Fig. 1).

The effects of sanguinarine on the spindle microtubules and the organization of the chromosomes in mitotic HeLa cells are shown in Fig. 2. In control cells, metaphase spindles were bipolar with a compact plate of condensed chromosomes (Fig. 2A,D). At a low concentration of sanguinarine (0.5 μM), a concentration that inhibited proliferation by 13%, the spindle microtubule and chromosome organizations were very similar to that of control cells, although a few chromosomes were not aligned at the metaphase plate (Fig. 2B,E). At concentrations above 0.5 μM, sanguinarine disrupted the spindle microtubules and induced abnormalities in the chromosome organization. For example, 1 μM sanguinarine, which inhibited cell proliferation by 35%, depolymerized the spindle microtubules substantially (Fig. 2C). Further, at this concentration, most of the spindles lost their bipolar

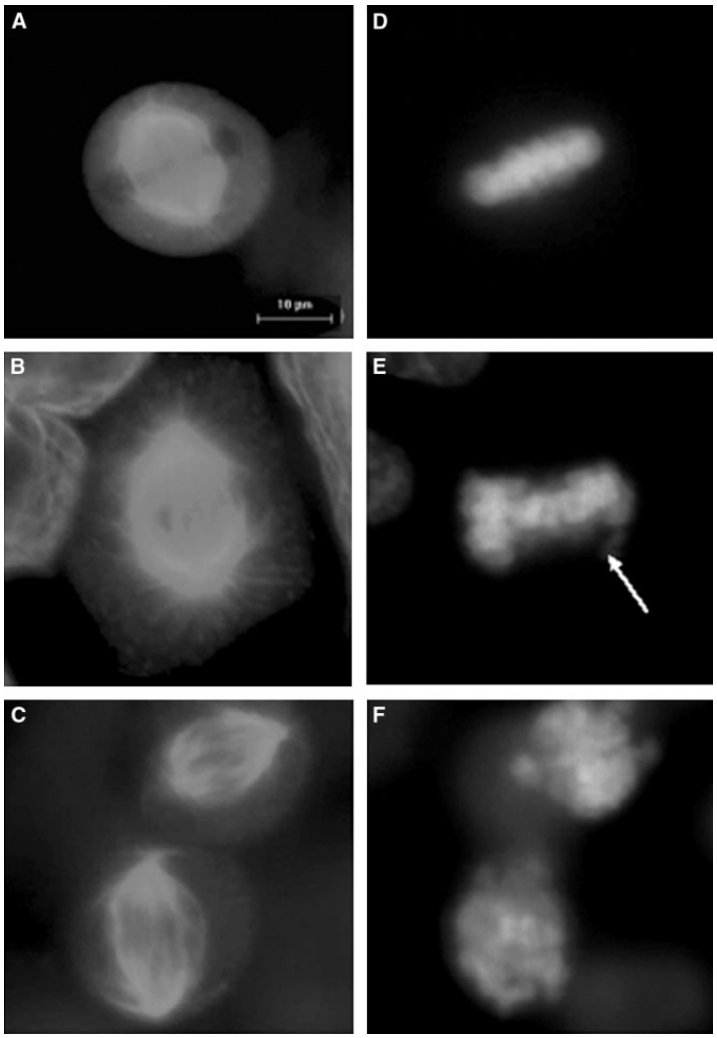

Fig. 2. Effects of sanguinarine on microtubule and chromosome organization of mitotic HeLa cells. HeLa cells were incubated with vehicle or different concentrations of sanguinarine for 20 h, and microtubules and chromosomes were visualized as described in Experimental procedures. Microtubules in the absence (A) and presence of 0.5 μM (B) and 1 μM (C) sanguinarine are shown. (D–F) Chromosome organization in the absence and presence of 0.5 μM and 1 μM sanguinarine, respectively.

organization, and the chromosomes became ball shaped (Fig. 2C,F).

Sanguinarine depolymerized interphase microtubules in a concentration-dependent manner (Fig. 3). For example, 1.5 μM sanguinarine depolymerized interphase microtubules significantly (Fig. 3B), 2 μM sanguinarine depolymerized interphase microtubules strongly (Fig. 3C), and 4 μM sanguinarine induced extensive depolymerization of interphase microtubules (Fig. 3D). In addition to depolymerizing the microtubules, sanguinarine also disorganized them. Specifically, it induced thick bundling of microtubules around the nucleus (Fig. 3C, arrows). Further, granulated aggregates of condensed tubulin were observed in the presence of 4 μM sanguinarine (Fig. 3D). The results show that the effective concentrations of sanguinarine required to inhibit HeLa cell proliferation are similar to those required to depolymerize interphase microtubules (Figs 1 and 3).

The effects of sanguinarine on the mitotic index were examined over a range of sanguinarine concentrations. The mitotic index was 2.8 ± 0.4% in the absence of sanguinarine, and 1.6 ± 0.3%, 1.3 ± 0.2%, and 0.6 ± 0.1% in the presence of 1, 2 and 3 μM sanguinarine, respectively, indicating that sanguinarine did not block cells at mitosis. Consistent with previous studies [22–24], we also found that sanguinarine induced cell death in a concentration-dependent manner (data not shown).

Sanguinarine inhibited HeLa cell proliferation irreversibly

In previous work [29], sanguinarine was thought to bind to tubulin covalently. We reasoned that, if binding of sanguinarine to tubulin is covalent, it would induce irreversible changes in cellular microtubule organization and function. To examine the

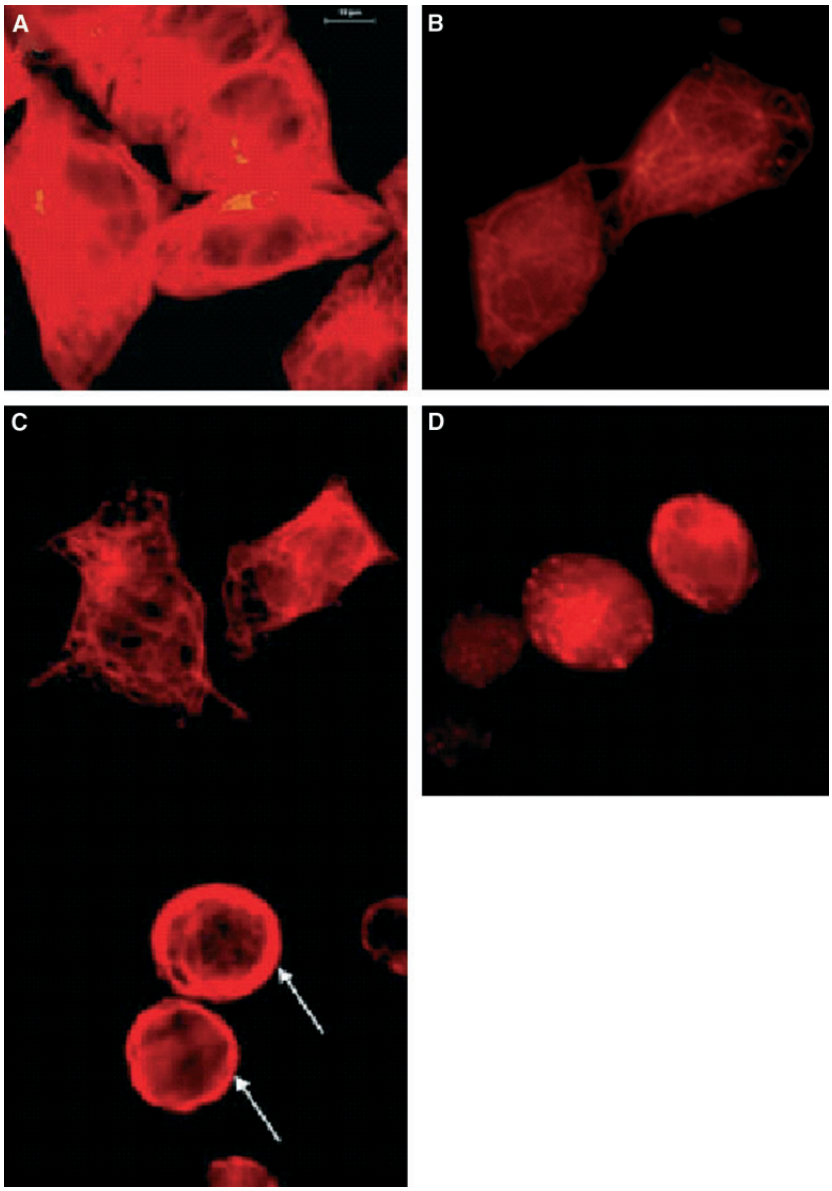

Fig. 3. Effects of sanguinarine on interphase microtubules. Interphase microtubules of HeLa cells are shown in the absence (A) and presence of 1.5 μM (B), 2 μM (C) and 4 μM (D) sanguinarine. Arrows indicate the bundling of interphase microtubules.

effects of a brief exposure of sanguinarine in HeLa cells, the cells were incubated with different concentrations of sanguinarine for 4 h. The medium was then removed and replaced with drug-free medium. The effects of the brief exposure of sanguinarine on the proliferation of HeLa cells were analyzed 20 h after drug removal. Sanguinarine inhibited cell proliferation with an IC_{50} of 1.5 ± 0.5 μM, indicating that the alkaloid exerted irreversible effects on its cellular targets (Fig. 4A). We also examined the effects of sanguinarine on microtubule organization 20 h after removal of the drug (Fig. 4B). Both mitotic spindle and interphase microtubules were significantly depolymerized, suggesting that sanguinarine permanently disrupted cellular microtubule assembly (Fig. 4B).

Effects of sanguinarine on tubulin polymerization

The effects of sanguinarine on microtubule polymerization were determined using two different tubulin preparations: phosphocellulose-purified tubulin and microtubule protein]tubulin and microtubule-associated protein (MAP)]. Using a light-scattering technique, Wolff & Knipling [29] found that sanguinarine inhibited tubulin assembly in the presence of paclitaxel. However, they did not provide data on the effects of sanguinarine on the amount of polymerized tubulin or

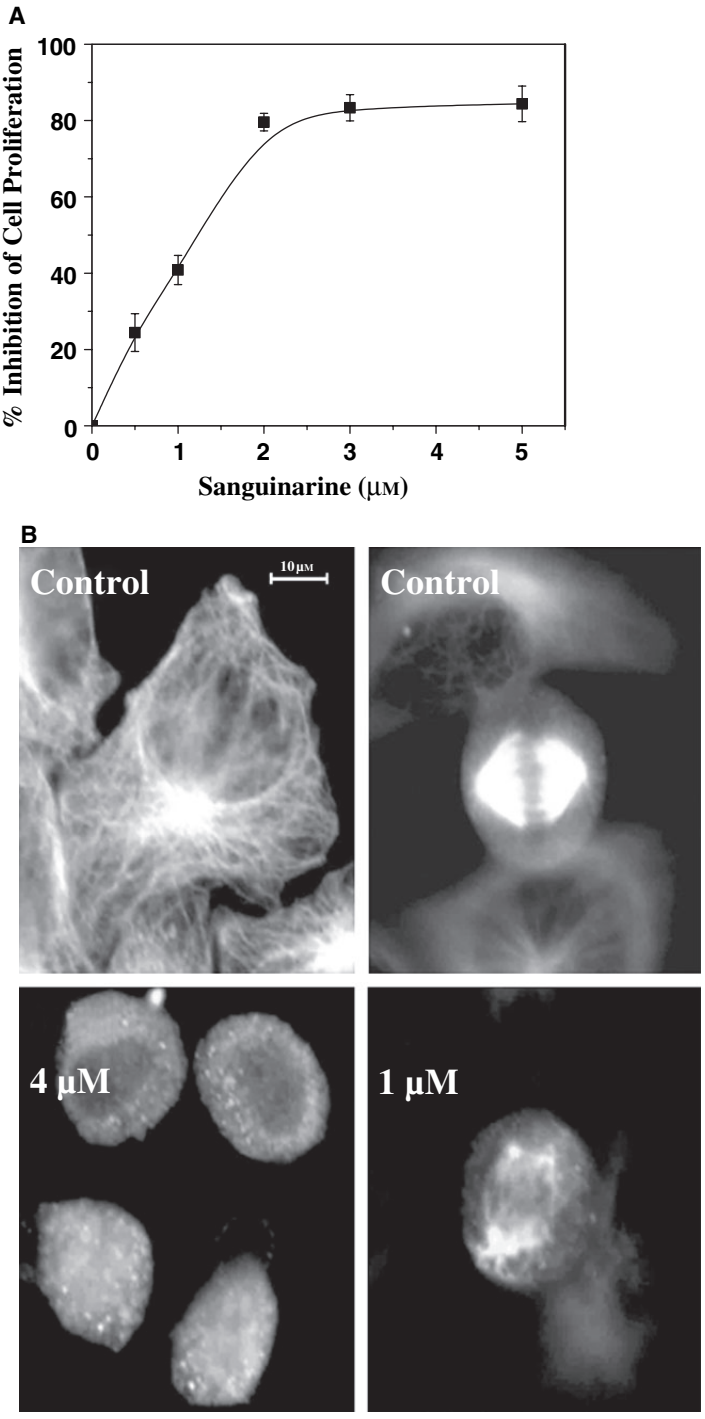

Fig. 4. Irreversible inhibitory effects of sanguinarine on HeLa cell proliferation (A) and microtubule organization (B). After incubation of HeLa cells with sanguinarine for 4 h, the sanguinarine-containing medium was replaced by fresh medium. The effects of the brief exposure of sanguinarine on the proliferation of HeLa cells and its microtubules were determined 20 h after the removal of the alkaloid.

on polymer morphology. Consistent with that study, in our study sanguinarine appeared to reduce the rate and extent of the paclitaxel-induced polymerization of tubulin, as measured by 90 ° light scattering (Fig. 5A). For example, 20 μm, 50 μM and 100 μM sanguinarine reduced the light scattering signal by 7%, 16%, and 40%, respectively (Fig. 5A). In contrast with its strong inhibitory effects on the light-scattering signal, sanguinarine reduced the amount of polymerized tubulin rather weakly (Fig. 5B). Specifically, 20 μM, 50 μM and 100 μM sanguinarine reduced the percentage of sedimentable polymer mass by 10%, 17% and 22%, respectively. Further, electron-microscopic analysis of the assembly reaction showed that 20 μM sanguinarine

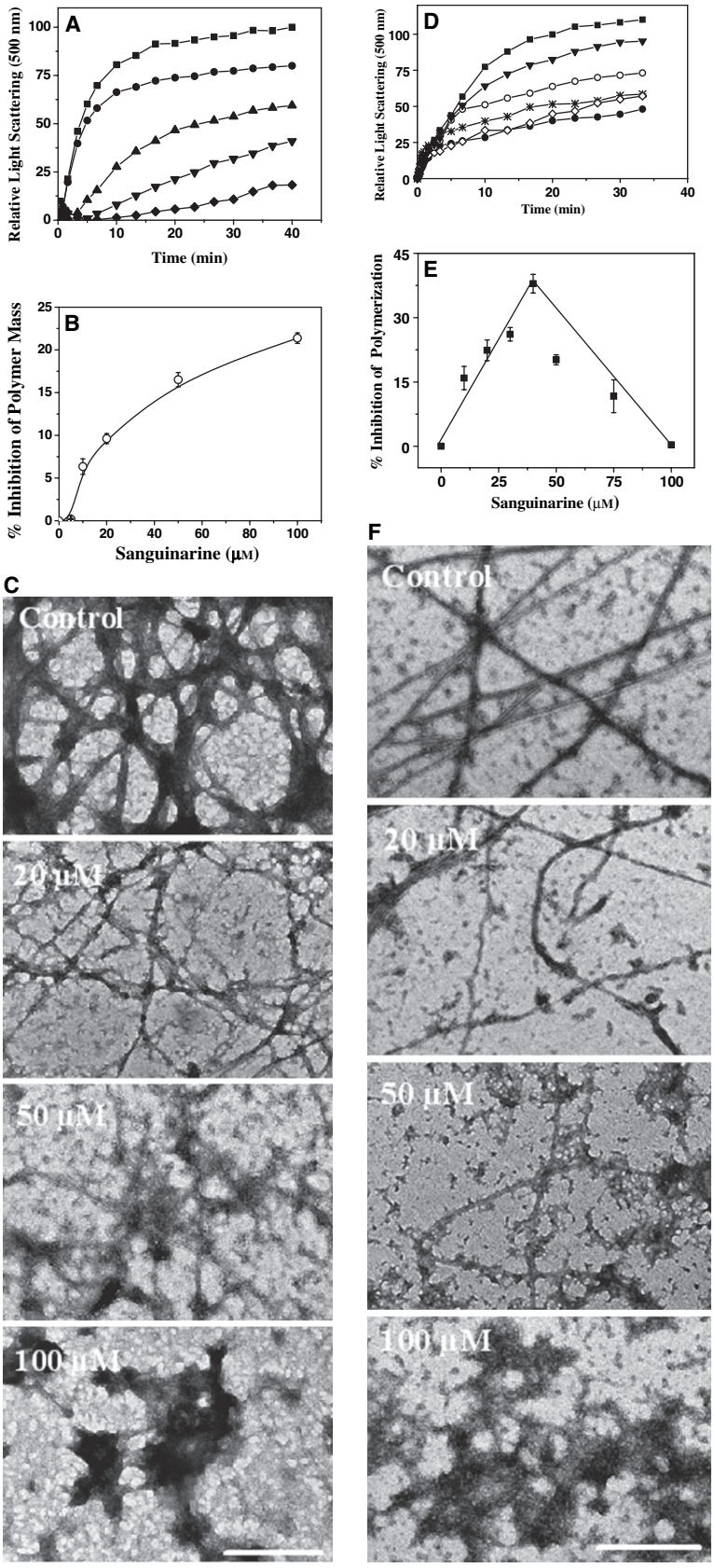

Fig. 5. Sanguinarine inhibited microtubule polymerization. Effects of sanguinarine on paclitaxel-induced tubulin polymerization (A–C). Paclitaxel-induced assembly of tubulin (10 μM) was monitored in the absence (■) and presence of 20 μM (●), 50 μM (▲), 75 μM (▼) and 100 μM (◆) sanguinarine by light scattering at 500 nm as described in Experimental procedures (A). The effects of sanguinarine on the sedimentable polymer mass are shown in (B). The experiment was performed four times. Each point represents the mean ± SD. Electron micrographs of microtubules in the absence and presence of 20, 50 and 100 μM sanguinarine are shown in (C). Images were taken at 43 000 × magnification using a Philips Fei Technai $G^2$12 electron microscope. The bar represents 500 nm. The effects of sanguinarine on the assembly of microtubule protein are shown in (D–F). Microtubule protein (1.5 mg·mL^{-1}) was polymerized in the absence and presence of different concentrations of sanguinarine. The assembly of microtubule protein in the absence (■) and presence of 20 μM (✱), 40 μM (●), 60 μM (◇), 75 μM (○) and 100 μM (▼) sanguinarine was monitored by light scattering at 500 nm (D). The graph shows the effect of sanguinarine on the polymer mass (E). Electron microscopic analysis of the assembly of microtubule protein in the absence and presence of sanguinarine is shown in (F). Images were taken at 43 000 × magnification. The bar represents 500 nm. The experiments were performed as described in Experimental procedures.

strongly reduced microtubule polymerization (Fig. 5C), and that high concentrations (50 and 100 μM) of sanguinarine altered polymer morphology (Fig. 5C).

Microtubule protein was polymerized in the absence or presence of different concentrations of sanguinarine. Similar to the effects of sanguinarine on the assembly of pure tubulin, the alkaloid inhibited the rate and extent of the assembly of microtubule protein, as measured by light scattering (Fig. 5D). For example, 20 μM sanguinarine decreased the extent of the light-scattering signal by 50%, and 40 μM sanguinarine inhibited the signal by 75%. However, increasing the concentration beyond 40 μM resulted in an increase in the light-scattering signal. For example, in the presence of 100 μM sanguinarine, the light-scattering signal was similar to that of the assembly of microtubule proteins in the absence of sanguinarine, indicating that at high concentrations sanguinarine either induced aggregation of tubulin or altered polymer morphology. The effect of sanguinarine on the assembly of microtubule protein was determined by sedimenting the polymers. Consistent with the scattering assay, low concentrations (40 μM) of sanguinarine inhibited the assembly of microtubule protein in a concentration-dependent manner. For example, 40 μM sanguinarine reduced the amount of polymerized microtubule protein by 40% (Fig. 5E). However, at higher concentrations, the inhibitory effect of sanguinarine on the assembled polymers was reversed, indicating that high concentrations of sanguinarine induced aggregation of tubulin in the presence of MAPs. Electron micrographs of polymers formed in the absence and presence of 20, 50 and 100 μM sanguinarine are shown in Fig. 5F. At 20 μM, sanguinarine clearly inhibited microtubule assembly, and microtubules were shorter than the control microtubules. High concentrations (50 and 100 μM) of sanguinarine induced extensive aggregation of microtubule proteins (Fig. 5F). Thus, the increase in the light-scattering signal and sedimentable polymer mass in the presence of high concentrations of sanguinarine appear to be due to the formation of aggregates of microtubule protein. The results indicate that sanguinarine induced aggregation of tubulin dimers in the presence of MAPs.

Sanguinarine copolymerized with tubulin into polymers

Tubulin was polymerized in the presence of different concentrations of sanguinarine, and the unbound sanguinarine was separated from the polymer-bound sanguinarine by sedimenting the polymers. The incorporation of sanguinarine per tubulin dimer into the polymer increased with increasing concentration of sanguinarine (Fig. 6). For example, the stoichiometries of sanguinarine incorporation per tubulin dimer in the polymer were 0.57 ± 0.1 and 1.1 ± 0.1 mol sanguinarine per mol tubulin in the presence of 10 and 20 μM sanguinarine, respectively. The results indicate that sanguinarine copolymerizes with tubulin into the tubulin polymers.

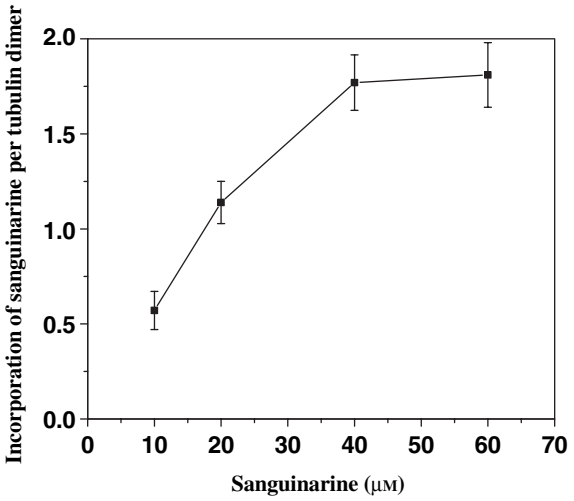

Fig. 6. Stoichiometry of incorporation of sanguinarine per tubulin dimer in microtubules. Tubulin (1.2 mg·mL^{-1}) was polymerized in buffer A containing 1 M glutamate and 1 mM GTP for 45 min at 37 °C in the presence of different concentrations (10–60 μM) of sanguinarine. Microtubules were spun down to separate free sanguinarine molecules from the polymer-bound sanguinarine. The stoichiometry of sanguinarine incorporation per tubulin dimer in the pelleted polymer was calculated as described in Experimental procedures. Each point represents the mean ± SD from three independent experiments.

Sanguinarine perturbed the secondary structure of tubulin

The effect of sanguinarine on the secondary structure of tubulin was examined by far-UV CD spectroscopy (Fig. 7). Sanguinarine altered the amplitude of the far-UV CD spectra of tubulin, indicating that it perturbed the secondary structure of tubulin.

Effects of sanguinarine on tubulin–1-anilinonaphthalene-8-sulfonic acid complex fluorescence

Hydrophobic fluorescence probes such as 1-anilinonaphthalene-8-sulfonic acid (ANS), bis-ANS and prodan are routinely used to determine ligand-induced conformational changes in tubulin [14]. Sanguinarine

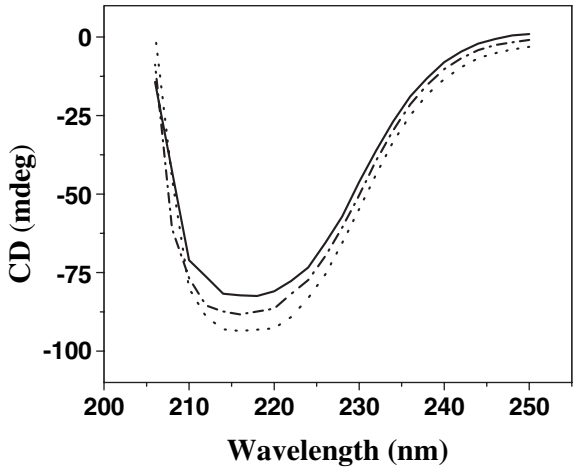

Fig. 7. Sanguinarine perturbed the secondary structure of tubulin. Tubulin (5 μM) in 25 mM Pipes buffer was incubated in the absence (dotted line) and presence of 10 μm (dash dot line) and 30 μM (solid line) sanguinarine for 30 min at 25 °C, and the far-UV CD spectra were recorded as described in Experimental procedures. The 222-nm CD signals of tubulin were found to be – (90 ± 1.1), – (82 ± 1.3) and – (77 ± 0.9) in the absence and presence of 10 and 30 μM sanguinarine, respectively. The intensities of the CD signal of tubulin at 222 nm in the absence and presence of sanguinarine were significantly different ($P < 0.01$). The experiment was repeated 5 times.

increased the fluorescence intensity of the tubulin–ANS complex up to a certain concentration (Fig. 8). For example, it was increased by 95% and 190% in the presence of 10 μM and 20 μM sanguinarine, indicating that sanguinarine induced conformational changes in tubulin. However, high concentrations of sanguinarine (> 20 μM) reduced the fluorescence intensity of the tubulin–ANS complex (Fig. 8). The results indicate the presence of at least two different types of sanguinarine-binding site on tubulin.

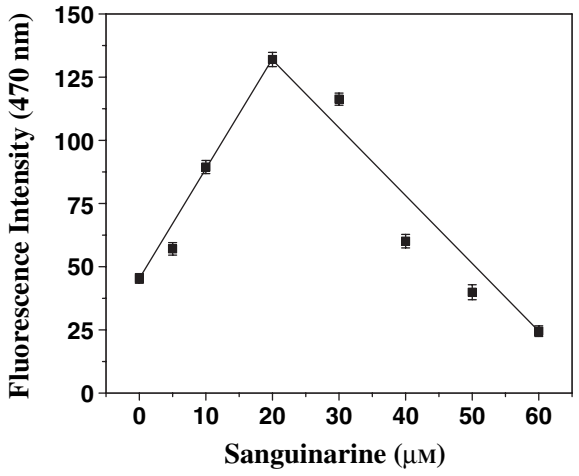

Fig. 8. Effects of sanguinarine on the fluorescence of the tubulin–ANS complex. The experiment was performed four times (mean ± SD).

Discussion

In this study, we found that sanguinarine inhibited proliferation of HeLa cells apparently by a depolymerizing effect on cellular microtubules. Further, sanguinarine bound to tubulin *in vitro* induced conformational changes in tubulin and inhibited polymerization of tubulin into microtubules. Microtubule-depolymerizing agents generally inhibit cell cycle progression at mitosis. Although sanguinarine depolymerized microtubules both *in vitro* and in cells, it did not induce mitotic block. The results suggest that the antiproliferative mechanism of action of sanguinarine is different from that of other microtubule-depolymerizing agents and that at least some microtubule/tubulin inhibitors can inhibit cell proliferation by a mechanism that does not involve mitotic arrest.

Sanguinarine inhibited HeLa cell proliferation and induced cell death without inhibiting mitosis. Therefore, in addition to microtubules, sanguinarine may have other cellular targets. Several mechanisms have been suggested to explain the antiproliferative activities of sanguinarine [22–28]. For example, it has been shown that sanguinarine perturbs several signaling pathways, including those operating through mitogen-activated protein kinase phosphatase-1 and NF-κB [22,26]. The role of microtubules in signal transduction and intracellular transport is widely accepted [4]. The results obtained in this study indicate that the modulation of the signaling pathways in cancer cells by sanguinarine may partly involve microtubule perturbation.

Sanguinarine depolymerized HeLa cell microtubules in a concentration range that was similar to that required to inhibit cell proliferation (Figs 2 and 3). At a concentration of 2 μM, sanguinarine inhibited cell proliferation by 70% and strongly depolymerized and disorganized the interphase microtubule network (Fig. 3). Several of the known microtubule-depolymerizing agents, including nocodazole, vinblastine, griseofulvin, cryptophycin-52, LY290181 and benomyl, inhibit cell proliferation by perturbing spindle organization and function in their lowest effective concentration range without detectably depolymerizing interphase microtubules [12–15]. For example, vinblastine inhibited HeLa cell proliferation by 50% with no apparent depolymerizing effects on interphase microtubules [13]. Similarly, 5 μM benomyl inhibited HeLa cell proliferation by 50% in the absence of any detectable

depolymerizing effects on interphase microtubules [14]. Interestingly sanguinarine, at its lowest effective concentration, significantly depolymerized and disorganized the interphase microtubule network (Fig. 3). In addition, a brief exposure of the cells to sanguinarine was sufficient to produce sustained depolymerization of the microtubules (Fig. 4B). Rather than increasing the percentage of mitotic cells, sanguinarine actually reduced the percentage of them, demonstrating that it does not induce mitotic block. Taken together, the results obtained in this report suggest that the loss of functional microtubules in sanguinarine-treated interphase cells may prevent these cells from progressing into mitosis. Similar modes of antiproliferative action have been reported for other antitubulin agents. For example, halogenated derivatives of acetamidobenzoyl ethyl ester were found to depolymerize microtubules and produce irreversible effects on cellular microtubules [16]. These agents block cell proliferation at the G_1/S phase of the cell cycle. Indanocine, a tubulin-binding drug, was also found to inhibit proliferation of certain kinds of cancer cell without arresting cells at mitosis [17].

Consistent with a previous report [29], sanguinarine was found to reduce the light-scattering signal associated with paclitaxel-induced tubulin polymerization (Fig. 5A). However, we found that sanguinarine only modestly reduced the amount of sedimentable tubulin polymer (Fig. 5B). For example, 100 μM sanguinarine reduced the light-scattering intensity of paclitaxel-induced tubulin assembly by 82%, whereas it reduced sedimentable polymer mass by only 22%. The results indicate that sanguinarine either altered polymer morphology or induced aggregation of tubulin dimers. Electron-microscopic analysis of the polymers showed that sanguinarine altered polymer morphology (Fig. 5C).

Sanguinarine exerted similar effects on the assembly of microtubule protein (tubulin plus MAPs) (Fig. 5D–F). At low concentrations (40 μM), it inhibited the assembly of microtubule protein in a concentration-dependent manner; however, high concentrations of sanguinarine induced aggregation of microtubule proteins, suggesting that sanguinarine induced tubulin aggregation in the presence of MAPs (Fig. 5D–F). In this study, we found that sanguinarine was incorporated with tubulin into the tubulin polymers (Fig. 6). The binding of sanguinarine to tubulin induced conformational changes in tubulin (Figs 7 and 8). Thus, the results suggest that the incorporation of a large number of conformationally altered tubulin dimers as tubulin–sanguinarine complexes into microtubules produced nonmicrotubule polymers.

A brief exposure of HeLa cells to sanguinarine was sufficient to inhibit cell proliferation irreversibly (Fig. 4A). In addition, the microtubule architecture and chromosome organization in the cells were found to be disrupted even 20 h after removal of the drug (Fig. 4B). It was previously suggested that sanguinarine covalently binds to tubulin by forming a pseudobase with the cysteine residues of tubulin [29]. In addition, we could not displace sanguinarine from the purified tubulin–sanguinarine complex by denaturing the preformed tubulin–sanguinarine complex using high concentrations (6 M) of guanidine hydrochloride, indicating that sanguinarine may bind to tubulin irreversibly (data not shown). Thus, the irreversible effects of sanguinarine in HeLa cells may be explained by its covalent binding to tubulin. Davis *et al.* [16] found that halogenated derivatives of acetamidobenzoyl ethyl ester inhibited proliferation of several types of cancer cell by depolymerizing microtubules without arresting cells at mitosis. Like sanguinarine, these agents were also thought to bind to tubulin covalently and were shown to exert irreversible effects on cells.

One of the major obstacles of effective drug action is the efflux of the drug after its entry into cells by protein pumps such as P-glycoprotein and multiple drug resistance protein 1 [30]. Sanguinarine was also found to be effective against multidrug-resistant HeLa cells [23]. As sanguinarine binds tightly to tubulin, it may be difficult for the efflux machinery to pump out the drug. Thus, the tight binding of sanguinarine to tubulin may be beneficial for cancer chemotherapy.

Experimental procedures

Materials

Sanguinarine chloride, GTP, Pipes, sulforhodamine B, Hoechst 33342, propidium iodide and mouse monoclonal antibody to α-tubulin were purchased from Sigma (St Louis, MO, USA). Phosphocellulose (P11) was purchased from Whatman (Maidstone, UK). Alexa Fluor 568-labeled goat anti-mouse IgG and ANS were purchased from Molecular Probes (Eugene, OR, USA). All other reagents were of analytical grade.

Cell culture and proliferation assay

HeLa cells were grown in minimal essential media (Himedia, Bangalore, India) supplemented with 10% (v/v) fetal bovine serum, kanamycin (0.1 $mg \cdot mL^{-1}$), penicillin G (100 $units \cdot mL^{-1}$), and sodium bicarbonate (1.5 $mg \cdot mL^{-1}$) at 37 °C in 5% CO_2 as described previously [14]. Sulforhodamine B assay was performed with some modifications [14].

Briefly, HeLa cells (1×10^4) were seeded in a poly lysine-coated 96-well plate and grown for 20 h. Then, different concentrations of sanguinarine were added to the wells, and cells were incubated for 20 h. The cells were then fixed with 10% trichloroacetic acid for 1 h, rinsed with water, air-dried, and stained with 0.4% sulforhodamine B in 1% acetic acid for 1 h. Cell proliferation was determined by measuring A_{550} with a microplate reader (Bio-Rad, Hercules, CA, USA). The percentage inhibition of HeLa cell proliferation in the presence of different concentrations of sanguinarine was determined by subtracting A_{550} of protein-bound sulforhodamine B at time zero from all the experimental data points [14]. The experiment was repeated four times in duplicate.

Immunofluorescence microscopy

HeLa cells were seeded on coverslips at a density of 1×10^5 cells·mL^{-1} and grown in the absence and presence of different concentrations of sanguinarine for 20 h [14]. Then, cells were fixed in 3.7% formaldehyde and permeabilized with ice-chilled methanol (−20 °C). Nonspecific binding sites were blocked by incubating the cells with 2% BSA in NaCl/P_i for 15 min, and the cells were incubated with mouse monoclonal antibody to α-tubulin (1 : 150 dilution) for 2 h at 37 °C. After incubation, cells were washed twice with 2% BSA/NaCl/P_i. Then, the cells were incubated with Alexa Fluor 568-labeled goat anti-mouse IgG (1 : 300 dilution) for 1 h at 37 °C. For staining the DNA, antibody-stained cells were incubated with 4′,6-diamidino-2-phenylindole (1 μg·mL^{-1}) for 20 s. Microtubules and chromosomes were observed using a Nikon eclipse TE-2000U microscope. The images were analyzed using Image-Pro Plus software. For studying the irreversible effects of sanguinarine, HeLa cells were treated with sanguinarine for 4 h and then sanguinarine was removed by replacing the sanguinarine-containing medium with fresh medium.

Determination of mitotic indices and live/dead cells

HeLa cells were treated with sanguinarine as described above. The percentage of interphase and mitotic cells was determined by Wright-Giemsa staining as described previously [14]. A minimum of 500 cells was counted per concentration of sanguinarine for each experiment. The experiment was performed four times, and the data are means of four independent experiments. To determine the number of live/dead cells by Hoechst 33342/propidium iodide (1 μg·mL^{-1}) double staining, cells were treated with sanguinarine for 20 h and then fixed with ice-cold methanol. Live and dead cells were identified by blue (Hoechst 33342) and red (propidium iodide) staining, under a fluorescence microscope [31].

Purification of tubulin

Goat brain tubulin (depleted of MAPs) was isolated by two cycles of polymerization and depolymerization in the presence of 0.4 M sodium glutamate and 10% (v/v) dimethyl sulfoxide [14]. Tubulin was purified from the MAP-depleted preparations by phosphocellulose chromatography and stored at −80 °C [14]. Microtubule protein (tubulin plus MAPs) was isolated by two cycles of polymerization and depolymerization in the presence of 4 M glycerol [32]. Tubulin concentration was determined by the method of Bradford [33], using BSA as a standard.

Spectral measurements

Absorbance and fluorescence measurements were performed using a V-530 UV-Visible spectrophotometer and a FP-6500 spectrofluorimeter (Jasco, Tokyo, Japan), respectively. Spectra were taken by multiple scans. A cuvette of 0.3 cm path length was used for all measurements. The CD spectra were recorded after incubating tubulin (5 μM) without or with different concentrations of sanguinarine over the range 250–195 nm in a Jasco J-810 spectropolarimeter at 25 °C, using a 0.1-cm path length cuvette [34].

Inhibition of paclitaxel-induced polymerization of tubulin

Purified tubulin (10 μM) was polymerized in buffer A (25 mM Pipes, pH 6.8, 1 mM EGTA and 3 mM $MgSO_4$) in the presence of 10 μM paclitaxel and 1 mM GTP with different concentrations (0–100 μM) of sanguinarine at 37 °C. The rate and extent of polymerization were monitored through 90 ° light scattering at 500 nm [35]. For the sedimentation assay, tubulin (10 μM) was polymerized as described above for 45 min at 37 °C. After polymerization, the samples were centrifuged at 30 °C for 40 min at 56 000 ***g***. The protein concentration in the supernatant was measured, and polymer mass was calculated by subtracting the supernatant concentration from the total protein concentration.

Transmission electron microscopy

Samples for electron microscopic analysis were prepared as described previously [14]. Briefly, microtubules were fixed with prewarmed 0.5% glutaraldehyde in buffer A for 5 min. Samples (20 μL) were applied to carbon-coated electron microscope grids (300-mesh) for 30 s and blotted dry. The grids were subsequently negatively stained with 1% uranyl acetate and air-dried. The samples were viewed using a Philips Fei Technai $G^2$12 electron microscope. Images were taken at 43 000 × magnifications. The

average number of microtubules per field of view was determined by counting the number of polymers per field.

Copolymerization of sanguinarine and tubulin

Tubulin (1.2 mg·mL^{-1}) was polymerized in buffer A containing 1 M glutamate and 1 mM GTP for 45 min at 37 °C in the presence of different concentrations (10–60 μM) of sanguinarine. Microtubules were spun down (52 000 ***g*** at 30 °C) to separate free sanguinarine molecules from the polymer-bound sanguinarine. The microtubule pellet was washed carefully and then dissolved in PEM (25 mM pipes, pH 6.8, 1 mM EGTA, 3 mM $MgSO_4$) buffer. The concentration of microtubule-bound sanguinarine was estimated by measuring A_{325}. The incorporation stoichiometry of sanguinarine per tubulin dimer in the polymer was calculated by dividing the concentration of the bound sanguinarine by the concentration of tubulin in the pellet. The nonspecific precipitation (background signal) of sanguinarine was estimated by incubating BSA (1.2 mg·mL^{-1}) with different concentrations (10–60 μM) of sanguinarine in the presence of GTP and magnesium for 30 min at 37 °C, and then sedimenting the reaction mixtures in exactly the same way as described for microtubule assembly. In the absence of microtubules, the amount of sanguinarine precipitated under identical experimental conditions was found to be negligible (1%). We used the amount of sanguinarine precipitated at each concentration of sanguinarine in the presence of BSA as a background to correct the experimental data.

Effects of sanguinarine on tubulin–ANS complex fluorescence

Tubulin (2 μM) in PEM buffer was incubated in the absence and presence of various concentrations (5–60 μM) of sanguinarine at room temperature for 10 min and then with 100 μM ANS for an additional 20 min. The fluorescence intensity was measured at 470 nm using 380 nm as an excitation wavelength [14].

Acknowledgements

We thank the Regional Sophisticated Instrumentation Centre, IIT Bombay for the use of their electron microscopy facility, and Dr Leslie Wilson, Dr Kamlesh Gupta, Manas Kumar Santra, K Rathinasamy and Renu Mohan for critical reading of the manuscript. The work is partly supported by grants (to D.P.) from the Department of Biotechnology, Board of Research in Nuclear Sciences, and Swarnajayanti Fellowship (DST) from the Government of India.

References

1 Lodish H, Berk A, Zipursky SL, Matsudaira P, Baltimore D & Darnell J (2000) *Molecular Cell Biology*. 4th edn. W.H. Freeman and company, New York.
2 Desai A & Mitchison TJ (1997) Microtubule polymerization dynamics. *Annu Rev Cell Dev Biol* **13**, 83–117.
3 McIntosh JR, Grishchuk E & West RR (2002) Chromosome–microtubule interactions during mitosis. *Annu Rev Cell Dev Biol* **18**, 193–219.
4 Gunderson GG & Cook TA (1999) Microtubules and signal transduction. *Curr Opin Cell Biol* **11**, 81–94.
5 Wilson L, Panda D & Jordan MA (1999) Modulation of microtubule dynamics by drugs: a paradigm for the actions of cellular regulators. *Cell Struct Funct* **24**, 329–335.
6 Downing KH (2000) Structural basis for the interaction of tubulin with proteins and drugs that affects microtubule dynamics. *Annu Rev Cell Dev Biol* **16**, 89–111.
7 Jordan MA (2002) Mechanism of action of antitumor drugs that interacts with microtubules and tubulin. *Curr Med Chem AntiCancer Agents* **2**, 1–17.
8 Jordan MA & Wilson L (2004) Microtubules as a target for anticancer drugs. *Nat Rev Cancer* **4**, 253–265.
9 Hamel E (1996) Antimitotic natural products and their interactions with tubulin. *Med Res Rev* **16**, 207–231.
10 Panda D, Jordan MA, Chu KC & Wilson L (1996) Differential effects of vinblastine on polymerization and dynamics at opposite microtubule ends. *J Biol Chem* **271**, 29807–29812.
11 Panda D, Singh JP & Wilson L (1997) Suppression of microtubule dynamics by LY290181. A potential mechanism for its antiproliferative action. *J Biol Chem* **272**, 7681–7687.
12 Panda D, DeLuca K, Williams D, Jordan MA & Wilson L (1998) Antiproliferative mechanism of action of cryptophycin-52: kinetic stabilization of microtubule dynamics by high-affinity binding to microtubule ends. *Proc Natl Acad Sci USA* **95**, 9313–9318.
13 Jordan MA, Thrower D & Wilson L (1991) Mechanism of inhibition of cell proliferation by Vinca alkaloids. *Cancer Res* **51**, 2212–2222.
14 Gupta K, Bishop J, Peck A, Brown J, Wilson L & Panda D (2004) Antimitotic antifungal compound benomyl inhibits brain microtubule polymerization and dynamics and cancer cell proliferation at mitosis, by binding to a novel site in tubulin. *Biochemistry* **43**, 6645–6655.
15 Panda D, Rathinasamy K, Santra MK & Wilson L (2005) Kinetic suppression of microtubule dynamic instability by griseofulvin: implications for its possible use in the treatment of cancer. *Proc Natl Acad Sci USA* **102**, 9878–9883.
16 Davis A, Jiang JD, Middleton KM, Wang Y, Weisz I, Ling YH & Bekesi JG (1999) Novel suicide ligands of

tubulin arrest cancer cells in S-phase. *Neoplasia* **1**, 498–507.
17 Leoni LM, Hamel E, Genini D, Shih H, Carrera CJ, Cottam HB & Carson DA (2000) Indanocine, a microtubule-binding indanone and a selective inducer of apoptosis in multidrug-resistant cancer cells. *J Natl Cancer Inst* **92**, 217–224.
18 Godowski KC (1989) Antimicrobial action of sanguinarine. *J Clin Dent* **1**, 96–101.
19 Beuria TK, Santra MK & Panda D (2005) Sanguinarine blocks cytokinesis in bacteria by inhibiting FtsZ assembly and bundling. *Biochemistry* **44**, 16584–16593.
20 Ahmad N, Gupta S, Husain MM, Heiskanen KM & Mukhtar H (2000) Differential anti-proliferative and apoptotic response of sanguinarine for cancer cells versus normal cells. *Clin Cancer Res* **6**, 1424–1428.
21 Slaninova J, Taborska E & Bochorakoa & Slanina J (2001) Interaction of benzophenanthridine and protoberberine alkaloids with animal and yeast cells. *Cell Biol Toxicol* **17**, 51–63.
22 Weerasinghe P, Hallock S & Liepins A (2001) Bax, Bcl-2, and NF-kappaB expression in sanguinarine induced bimodal cell death. *Exp Mol Pathol* **71**, 89–98.
23 Ding Z, Tang SC, Weerasinghe P, Yang X, Pater A & Liepins A (2002) The alkaloid sanguinarine is effective against multidrug resistance in human cervical cells via bimodal cell death. *Biochem Pharmacol* **63**, 1415–1421.
24 Adhami VM, Aziz MH, Mukhtar H & Ahmad N (2003) Activation of prodeath Bcl-2 family proteins and mitochondrial apoptosis pathway by sanguinarine in immortalized human HaCaT keratinocytes. *Clin Cancer Res* **9**, 3176–3182.
25 Adhami VM, Aziz MH, Reagan-Shaw SR, Nihal M, Mukhtar H & Ahmad N (2004) Sanguinarine causes cell cycle blockade and apoptosis of human prostate carcinoma cells via modulation of cyclin kinase inhibitor-cyclin-cyclin-dependent kinase machinery. *Mol Cancer Ther* **3**, 933–940.
26 Vogt A, Tamewitz A, Skoko J, Sikorski RP, Giuliano KA & Lazo JS (2005) The benzo[c]phenanthridine alkaloid, sanguinarine, is a selective, cell-active inhibitor of mitogen-activated protein kinase phosphatase-1. *J Biol Chem* **280**, 19078–19086.
27 Eun JP & Koh GY (2004) Suppression of angiogenesis by the plant alkaloid, sanguinarine. *Biochem Biophys Res Commun* **317**, 618–624.
28 Dvorak Z, Vrzal R, Maurel P & Ulrichova J (2006) Differential effects of selected natural compounds with anti-inflammatory activity on the glucocorticoid receptor and NF-kappaB in HeLa cells. *Chem Biol Interact* **159**, 117–128.
29 Wolff J & Knipling L (1993) Anti-microtubule properties of Benzophenanthridine alkaloids. *Biochemistry* **32**, 1334–1339.
30 Legrand O, Simonin G, Perrot JY, Zittoun R & Marie JP (1998) Pgp and MRP activities using calcein-AM are prognostic factors in adult acute myeloid leukemia patients. *Blood* **91**, 4480–4488.
31 McKeague AL, Wilson J & Nelson J (2003) Staurosporine-induced apoptosis and hydrogen peroxide-induced necrosis in two human breast cell lines. *Br J Cancer* **8**, 125–131.
32 Panda D & Bhattacharyya B (1992) Excimer fluorescence of pyrene-maleimide-labeled tubulin. *Eur J Biochem* **204**, 783–787.
33 Bradford MM (1976) A rapid and sensitive method for the quantitation of microgram quantities of proteins utilizing the principle of protein-dye binding. *Anal Biochem* **72**, 248–254.
34 Gupta K & Panda D (2002) Perturbation of microtubule polymerization by quercetin through tubulin binding: a novel mechanism of its antiproliferative activity. *Biochemistry* **41**, 13029–13038.
35 Gaskin F, Cantor CR & Shelanski ML (1974) Turbidimetric studies of the *in vitro* assembly and disassembly of porcine neurotubules. *J Mol Biol* **89**, 737–755.